

Received March 28, 2017; reviewed; accepted June 03, 2017

Effect of modified starch on separation of fluorite from barite using sodium oleate

Zhijie Chen ¹, Zijie Ren ^{1,2}, Huimin Gao ^{1,2}, Yupeng Qian ^{1,2}, Renji Zheng ¹

¹ Wuhan University of Technology, School of Resources and Environmental Engineering, Wuhan 430070, China

² Hubei Key Laboratory of Mineral Resources Processing & Environment, Wuhan 430070, China

Corresponding author: rzj424711087@163.com (Zijie Ren)

Abstract: In this study, a modified starch was utilized to selectively separate barite from fluorite. The results of flotation tests showed that highly selective separation of fluorite from barite was obtained when 250 mg/dm³ of modified starch and 13.16×10⁻⁵ mol/dm³ sodium oleate was used in neutral solutions. FTIR spectra results showed that the modified starch can adsorb on the fluorite and barite surfaces. Zeta potential analyses indicated that the modified starch had little effect on adsorption of sodium oleate on the fluorite surface, although it interfered with the adsorption of sodium oleate on the barite surface. Contact angle measurements results corresponded well with the flotation results.

Keywords: fluorite, barite, modified starch, flotation

1. Introduction

Fluorite is in high demand nowadays as the primary resource of fluorine in chemical manufacturing, glass industry and ceramic industry (Gao et al., 2016). In addition, most of fluorite ore deposits are composed of multiple substances and are hard to treat. Thus, achieving fluorite of high-grade purity is an urgent task in mineral processing.

Fluorite mineral is closely associated with barite, and needs to be distinguished from barite through beneficiation. Separation of fluorite from barite has been extensively explored over the past years in China (Bi et al., 2015; Yu, 2015), with the results having suggested that flotation is the most efficient means. However, separation by flotation is problematic, because of their similar responses to collectors (Hu et al., 2003), which makes it imperative to find a suitable inhibitor scheme. Among common inhibitors, starch distinguishes itself primarily for its high abundance, ready availability, low cost and environmental friendliness (Li et al., 2010). Nevertheless, starch cannot selectively depress barite in the presence of fluorite, according to the preceding flotation results (Hanna, 1974; Bi et al., 2015). Hence, it is worth further developing starch to improve its separation efficiency.

It was noted that ferric salt (Fe³⁺) can heighten the floatability of fluorite (Zhang et al., 2015) and barite (Lu, 2010) using sodium oleate as a collector. Zhang et al. (2015) examined the activation mechanism of Fe³⁺ in fluorite flotation and the results showed that iron hydroxide (Fe(OH)₃) was the major active component in flotation in the appropriate pH range (pH 6-8). Lu (2010) found that Fe³⁺ activated barite through generation of hydroxylated complex or hydroxide sediments on the barite surface. However, the regulation degree of ferric salt on the floatability of fluorite and barite is different (Yu, 2015). From this perspective, ferric salt may be a selective activator in separation of fluorite and barite.

In this study, starch was modified with a ferric salt, with the subsequent modified starch (MS), and then evaluated with single mineral flotation tests and binary mixed mineral flotation tests. The depression mechanism has been investigated by FTIR spectra analyses, zeta potential measurements and contact angle measurements.

2. Experimental

2.1 Minerals and reagents

Hand-picked fluorite and barite samples were collected from Chongqing, China. The purities of fluorite and barite were over 97% based on X-ray diffraction (Fig. 1) and chemical analysis (Table 1). It can be noticed that the characteristic peaks of fluorite and barite powder samples corresponding to the standard spectra of fluorite (JCPDS card No. 35-0816) and barite (JCPDS card No. 24-1035) very well. The samples were ground in a porcelain ball mill and then dry-screened to obtain particles with a size ranging from -80 to +38 μm , which were used for micro-flotation tests. Samples used for infrared spectrum and zeta potential measurements were achieved by further grinding of the -80 and +38 μm particles. The high-grade lumps of fluorite and barite ore were cut into disks about 10 mm long, 10 mm wide and 5 mm thick, which were used for contact angle measurements.

Several researches showed that flotation reagent species would dominantly adsorb on the commonly exposed surfaces of certain minerals (Gao et al., 2012; Gao et al., 2015b; Kou et al., 2016). The commonly exposed surface of fluorite is (111), while (001) and (210) surfaces for barite based on the previous studies (Gao et al., 2014; Gao et al., 2015a; Ren et al., 2017). According to the XRD results in Fig. 1, it is obvious that the mainly exposed surfaces of fluorite and barite are (111) and (210), respectively. That is to say, the (111) surface of fluorite crystal acts as the main adsorption sites in the flotation process, and (210) surface for barite. In order to validate that the contact angle measurements could represent the flotation process, XRD analysis on the high grade lumps was conducted and the results are shown in Fig. 1. The results shows that only the (111) surface of fluorite lump was exposed. While for barite lump, the main exposed surface was the (210) surface, which consists with the powder samples. It means the surface properties of fluorite and barite minerals are mainly governed by the properties of (111) and (210) cleavage surfaces, respectively, in the contact angle measurements.

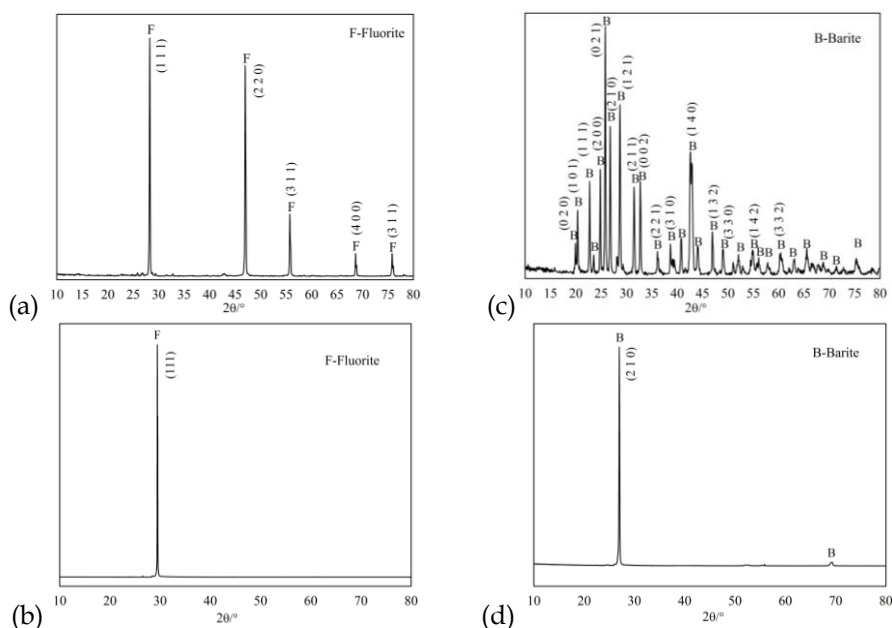


Fig. 1. XRD spectra of fluorite and barite samples (a) fluorite powder, (b) fluorite slump, (c) barite powder, (d) barite slump

Analytical grade hydrochloric acid and sodium hydroxide were prepared as 1% solutions for pH adjustment, with chemical grade sodium oleate (NaOL) acting as a collector. Modified starch (MS), which was a mixture of soluble starch (analytical-grade, 10 grams), ferric chloride hexahydrate (analytical-grade, 1 gram) and ultrapure water (0.3 dm^3) (Yu et al., 2016), was utilized as an inhibitor. The preparation process of MS is given as follow: firstly, 10 grams soluble starch, 1 grams ferric chloride and 0.3 dm^3 ultrapure water was mixed in a beaker; next, it was continuously stirred (300 r/min) at 85-90 $^{\circ}\text{C}$ until the color of the solution was reddish-brown. Deionized water with a

resistivity value of $18.25 \text{ M}\Omega \cdot \text{cm}$ was used throughout the experiments and spectroscopic-grade KBr was applied in FTIR spectra measurement.

Table 1. Chemical composition of fluorite and barite powder samples (%)

Mineral	SO ₃	CaO	Cl	BaO	MgO	Al ₂ O ₃	SiO ₂	CeO	F	Na ₂ O	LOI
Fluorite	0.19	50.78	0.09	0.24	0.04	0.01	0.22	0.05	47.59	-	0.79
Barite	33.63	1.34	0.02	64.18	0.13	0.01	0.19	-	0.02	0.18	0.30

*Loss-on-ignition

2.2 Microflotation tests

The microflotation tests were conducted with a RK/ FGC- 35 flotation machine. The particles (2.0 g) were placed into a Plexiglas cell, which was then filled with a certain amount of deionized water. The pulp was continuously stirred at 1600 rpm for 2 min using a pH regulator and 2 min with the depressant, before the collector was introduced and the pulp was conditioned for 2 min. During these steps, temperature was controlled to be about $20 \pm 2 \text{ }^\circ\text{C}$. The pH of the slurry was monitored before flotation, followed by flotation for 5 min. For single mineral flotation, the floated and tailing fractions were collected separately and dried, before being weighed for calculation. For artificially mixed minerals flotation, the concentrates and tailings were assayed (Chinese standards GB/T 5195.1-2006) to acquire the grades of fluorite and barite, before calculated the recovered amount.

2.3 FT-IR spectra

The infrared spectra were recorded by NEXUS Fourier transform infrared spectrometer of Thermo Nicolet Company in the $4000\text{-}500 \text{ cm}^{-1}$ region through KBr disks. 2.0 g of mineral samples were mixed with a certain amount of deionized water and reagents corresponding to the flotation test. After that, the suspension was stirred for 10 min, and then settled for 10 min. Later, the solution was filtered. The treated sample was first dried in a vacuum desiccator at room temperature, before a tiny amount of the dried powder was used for FTIR measurement.

2.4 Zeta potential measurements

Zeta potential were measured by 90 Plus Zeta Size Analyzer (Brookhaven Instruments Corporation, USA). The particle size of the ground powder was finer than $2 \text{ }\mu\text{m}$ ($D_{98}=1.864 \text{ }\mu\text{m}$, detected by BT-9300S laser particle size distribution instrument) for zeta potential measurement tests. The suspensions (0.1% mass fraction) with $1.00 \times 10^{-3} \text{ mol/dm}^3$ KCl solution were dispersed in a beaker, before being magnetically stirred for 10 min with and without flotation reagents at various pH values. After 5 min, the supernatant was obtained for zeta potential measurements. Each sample was measured three times and the mean values were reported.

2.5 Contact angle measurements

Contact angles were measured by a JC2000C1 contact angle goniometer (Shanghai Powereach Digital Technology Equipment Co. Ltd.) using the sessile drop method. Before every single measurement, the mineral disks were polished by metallographic sandpaper, and then washed with deionized water. The prepared mineral blocks were conditioned with the same flotation reagent regime as the flotation tests. After this, they were air-dried and tested. For each sample, five drops were measured and the average value was determined.

3. Results and discussion

3.1 Flotation results of single mineral

3.1.1 Flotation of fluorite and barite without MS

The effect of pH on the flotation behavior of fluorite and barite is illustrated in Fig. 2. The results stated that the recoveries of both fluorite and barite increased drastically when pH was increased from 3 to 5, with there still being relatively high levels in recoveries of two minerals in the pH range of 7-11. Beyond this pH range, recovery curves of both fluorite and barite decreased slightly. The

maximum recovery of fluorite (92.35%) was reached at a pH of 8, while that of barite (91.94%) occurred at a pH of 9. As observed, fluorite showed a similar flotation response to barite in the pH range of 5- 13.

The flotation response of fluorite and barite as a function of sodium oleate dosage is plotted in Fig. 3. An increase in the sodium oleate concentration had a positive influence on the recoveries of both fluorite and barite when the pH was fixed at 7. The recoveries of both fluorite and barite increased rapidly when the sodium oleate concentration was increased from 3.29×10^{-5} to 13.16×10^{-5} mol/dm³, reaching the maximum of 94.32 and 91.14%, respectively. With a further increase in the sodium oleate dosage, the recoveries of both fluorite and barite remained stable.

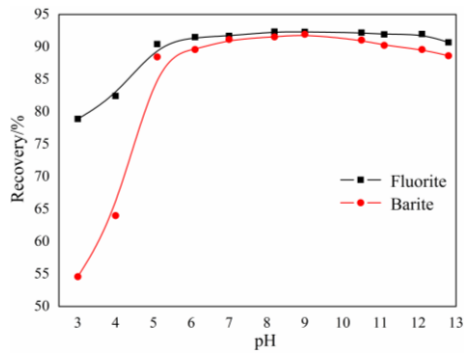


Fig. 2. Effect of pH on recovery of fluorite and barite in the absence of MS ($c_{NaOL} = 1 \times 10^{-4}$ mol/dm³)

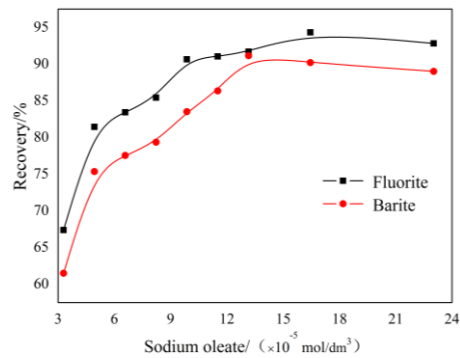


Fig. 3. Effect of NaOL dosage on recovery of fluorite and barite in the absence of MS (pH= 7)

According to the above results, it is apparent that the flotation recovery curves of fluorite and barite seem to be parallel in most cases. Thus, it is hard to separate fluorite from barite using sodium oleate as a collector without an inhibitor.

3.1.2 Flotation of fluorite and barite with MS

The flotation response of fluorite and barite in the presence of MS with different concentrations was considered, and the results are presented in Fig. 4. Fig. 4 clearly illustrates that the usage of MS had a marked inhibition on barite while having negligible effect on the fluorite recovery.

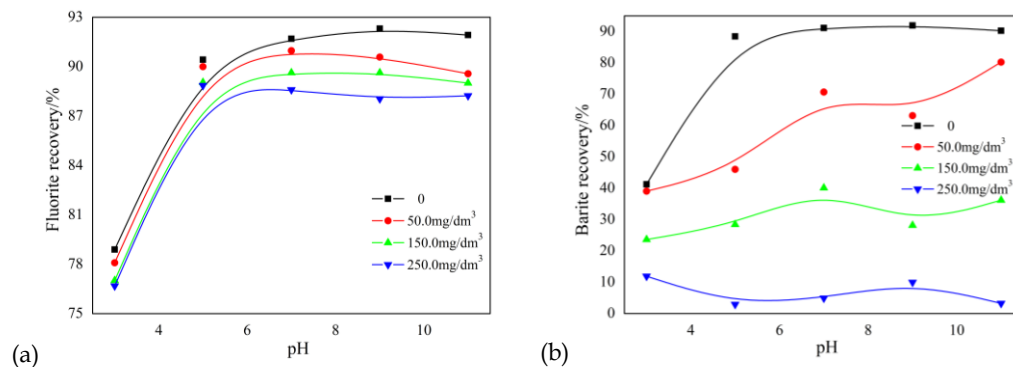


Fig. 4 Effect of MS on flotation recovery of fluorite (a) and barite (b) with different concentration ($c_{NaOL} = 13.16 \times 10^{-5}$ mol/dm³)

For fluorite (Fig. 4a), the flotation recovery decreased slightly as the concentration of MS increased from 0 to 250.0 mg/dm³, whereas in the case of barite (Fig. 4b), there was a noticeable reduction. MS was able to reduce the recovery of barite dramatically in the pH range of 3- 11, especially when the consumption exceeded 50.0 mg/dm³. The recovery of barite was less than 10% with 250.0 mg/dm³ of MS in the pH region of 5 to 11. In the presence of 250 mg/dm³ of MS at a pH of 7, the recoveries of fluorite and barite were 88.59 and 4.92%, respectively. It may be a suitable strategy to separate fluorite from barite.

3.2 Flotation of artificial mixed minerals

Flotation tests on artificially mixed minerals of fluorite (1.0 g) and barite (1.0 g) were conducted to test MS and the results are summarized in Table 2. It was clearly seen that the concentrate contained 89.07% fluorite with a low barite contaminations, with the recovery of fluorite being 84.62% while that of barite was 10.38%. In the tailing, the recovery of barite was 89.62% with a grade of 85.35%. Obviously, the effectual separation of fluorite from barite is possible using MS as a depressant.

Table 2. Flotation results on artificial mixed minerals with the reagent scheme of MS (250 mg/dm³) + NaOL (13.16×10⁻⁵ mol/dm³) at pH 7

Product	Yield, %	Grade, %		Recovery, %	
		Fluorite	Barite	Fluorite	Barite
Concentrate	47.5	89.07	10.93	84.62	10.38
Tailing	52.5	14.65	85.35	15.38	89.62
Total	100.00	50.00	50.00	100.00	100.00

3.3 FTIR spectrum analyses

FTIR spectroscopic analyses were conducted to examine the interaction of MS with the fluorite and barite surfaces. To examine the difference between MS and soluble starch, the spectra of MS and soluble starch were detected and the results are shown in Fig. 5.

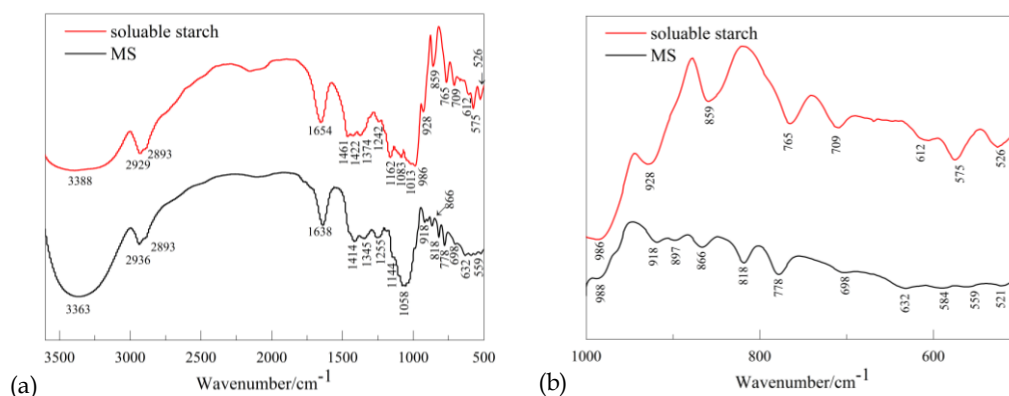


Fig. 5. FTIR spectra of MS and soluble starch in 4000-500 cm⁻¹(a) and 1000-500 cm⁻¹ (b)

In the spectrum of MS (Fig. 5(a)), the broad band around 3363 cm⁻¹ is assigned to the -OH stretching vibration, while the frequencies at 2936 cm⁻¹ and 2893 cm⁻¹ are attributed to the alkyl groups (Xia et al., 2009; Li et al., 2010; Kar et al., 2013). The band recorded at 1638 cm⁻¹ is explained by the vibration of bound water molecules (Kar et al., 2013). Several bands occurring in 1450- 1000 cm⁻¹ corresponds to CH, CH₂ in plane bending and C-O-H vibration, while frequencies in 1500- 1200 cm⁻¹ are assigned to the coupled mode of vibration due to hydrogen atoms (Kar et al., 2013). Bands near 1000 cm⁻¹ are due to the presence of C- OH stretching vibration and C- H bending vibration (Kar et al., 2013). Several bands located at 1000- 700 cm⁻¹ are assigned to the atomic group involved in the anomeric form (Xia et al., 2009). Compared with soluble starch, almost all the characteristic peaks of MS shifted obviously, so the structure of natural starch has changed. These phenomena result from the addition of ferric salt. To further compare the spectra, the 1000- 500 cm⁻¹ parts were enlarged, and the results are shown in Fig. 5(b). In the 1000- 500 cm⁻¹ parts, several new bands (897 cm⁻¹, 818 cm⁻¹, 698 cm⁻¹, 632 cm⁻¹, 559 cm⁻¹) appeared in MS except from the apparent shift of those peaks in natural starch. The band at 897 cm⁻¹ is due to Fe-O-H bending vibration (Gotić M and Musić S, 2007), the band at 698 cm⁻¹ can be assigned to Fe-O bonding (Komulainen S., et al. 2013; Kar B, et al., 2013), the bands at 632 cm⁻¹ and 559 cm⁻¹ can be assigned to Fe-O stretching vibrations (Cambier P., 1986; Gotić M and Musić S, 2007; Wang, 2013). These results indicates that ferric chloride hexahydrate reacts with natural starch might through chemical bonding.

The spectra of MS, fluorite and fluorite treated with MS are shown in Fig. 6. After treated with MS, several new peaks occurred compared with the pure fluorite spectrum. The frequencies at 2925 cm^{-1} , 2844 cm^{-1} , 1385 cm^{-1} and 930 cm^{-1} are assigned to alkyl groups in MS, while the peak located at 1025 cm^{-1} is caused by the presence of C-OH stretching vibration (Kar et al., 2013). The intensity at 1654 cm^{-1} is increased and the peak value shifts to 1641 cm^{-1} , demonstrating that MS has strong adsorption on the fluorite surface. The bands that are due to the -OH characteristic stretching of MS (1345 cm^{-1} , 1638 cm^{-1} and 3363 cm^{-1}) undergo an obvious shift, revealing the MS-fluorite interaction may occur through their hydroxyl groups, possibly by forming hydrogen bonds (Li et al., 2010). The frequencies located at 1058 cm^{-1} (C-H stretching vibration), 1144 cm^{-1} (C-O, C-H stretching vibration), 1414 cm^{-1} (CH_2 bending vibration, C-O-O stretching vibration), 2893 cm^{-1} and 2936 cm^{-1} (CH_2 , CH_3 stretching vibration) in MS have shifted to 1083 cm^{-1} , 1152 cm^{-1} , 1431 cm^{-1} , 2844 cm^{-1} and 2925 cm^{-1} , respectively. This indicates that MS was adsorbed on fluorite surface through chemical bonding (Xu et al., 2013; Xu et al., 2016). To summarize, the adsorption of MS on fluorite surface occurs via the formation of hydrogen bonds and chemical bonding.

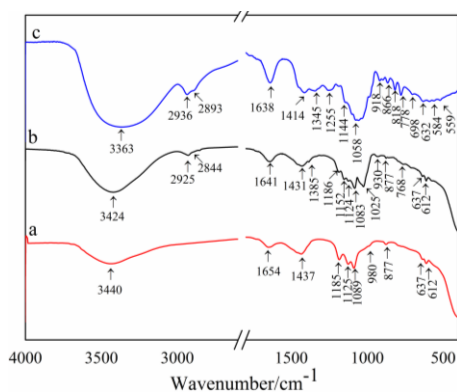


Fig. 6. Infrared spectra of fluorite (a), fluorite after being treated by MS (b) and MS (c)

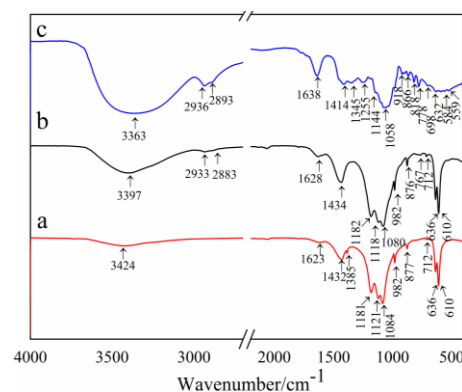


Fig. 7. Infrared spectra of barite (a), barite after being treated by MS (b) and MS (c)

The spectra of MS, barite and barite treated with MS are shown in Fig. 7. The characteristic bands of barite occur at 1181 cm^{-1} , 1084 cm^{-1} , 982 cm^{-1} and 630 cm^{-1} and 610 cm^{-1} . Frequencies at 1181 cm^{-1} and 1084 cm^{-1} are assigned to the asymmetric stretch vibration of SO_4^{2-} . Frequency at 982 cm^{-1} is due to the symmetric stretch vibration of SO_4^{2-} . In contrast, frequencies at 632 cm^{-1} and 610 cm^{-1} are from the bending vibrations of SO_4^{2-} (Wen, 1989). With the adsorption of MS, new bands are observed at 2933 cm^{-1} and 2883 cm^{-1} , which might be attributed to the alkyl groups in MS, illustrating that MS has adsorbed on the barite surface. Moreover, several bands in Fig. 7b due to the vibration of OH have an obvious shift compared with MS, which may be due to the formation of hydrogen bonds between barite and MS. Similar to Fig. 6, it can be conferred from Fig. 7 that the interaction between MS and barite surface occurs via the formation of hydrogen bonds and chemical bonding.

3.4 Zeta potential measurements results

To further uncover the selective depression mechanism of MS, zeta potentials of fluorite and barite in the absence and presence of flotation reagents were measured and the results are depicted in Fig. 8.

Fig. 8 shows that the IEPs (iso-electric points) of pH of 9.7 and pH of 4.6 were obtained for fluorite and barite, which are in the range of previous reports (Lu, 2008; Ucar A, 2013; Gao et al., 2015 (a); Gao et al., 2016; Wang et al., 2016; Ren et al., 2017; Chen et al., 2017). Moreover, both fluorite and barite exhibited positive potentials at pH values below the IEPs and negative potentials above the IEPs. It can be seen that NaOL has an obvious effect on the fluorite and barite surfaces. At a pH of 7, a greater decrease of 52 mV can be observed in Fig. 8a, compared with 31 mV for barite in Fig. 8b. The results implied that NaOL can have stronger interactions with the fluorite surface than barite surface at a pH of 7, which is consistent with the flotation results in Fig. 3. The species distribution diagram of oleate ions is portrayed in Fig. 9. It can be seen that $\text{RCOOH}_{(l)}$ is the main component in the pH range 0-8.40. When the pH is above 8.4, the negatively charged RCOO^- and $(\text{RCOO})_2^{2-}$ are the dominant species.

Fig. 8 indicates that oleate species can adsorb on both fluorite and barite surfaces in a wide pH range, even if the mineral surface is negatively charged. According to the flotation results and zeta potential measurement results, it can be concluded that NaOL can be adsorbed on a mineral surface through chemical interactions, instead of electrostatic interactions, which is consistent with previous studies (Rao K et al., 1991; Lu, 2008; Nunes A, et al., 2011; Gao et al., 2017).

The addition of MS has a positive impact on the zeta potentials of fluorite and barite, illuminating that MS can adsorb on fluorite and barite surface easily, but the extent is different. For fluorite, MS promotes the zeta potential so obvious that the average improvement is about 21 mV in the pH range of 3-11. In the case of barite, the average improvement is about 6 mV. These results indicated that the interaction between MS and fluorite is stronger than that of barite. Previous studies showed that starch can decrease the zeta potential of fluorite and barite (Hanna H S, 1974; Yu, 2015), which is distinct from the results of this research, indicating that positively charged species (ferric species) in MS were adsorbed on mineral surface. Moreover, it can be reasoned that the interaction between ferric species in MS and fluorite is stronger than that of barite. In addition, fluorite surface with higher positive zeta potential is more attractive to oleate species than barite surface, which is beneficial for the selective separation. It can be possible to reason out that the ferric species in MS act as a selective regulator during the separation of fluorite and barite.

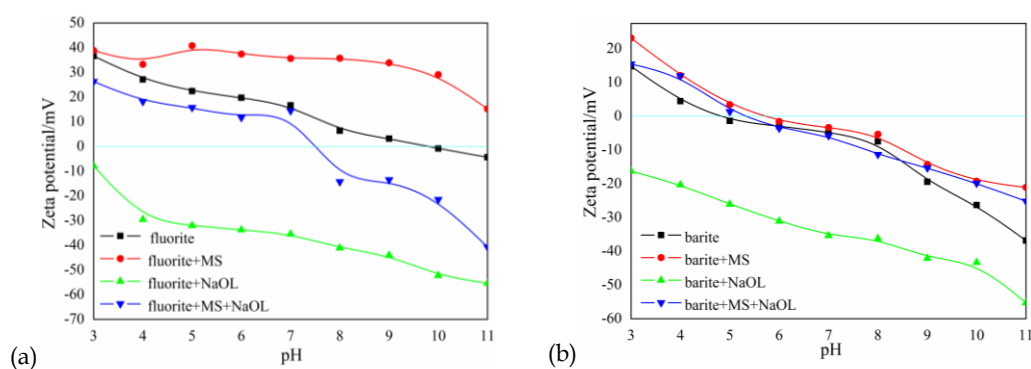


Fig. 8. Zeta potentials of fluorite (a) and barite (b) in the presence and absence of different flotation reagents ($c_{MS}=250 \text{ mg/dm}^3$, $c_{NaOL}=13.16 \times 10^{-5} \text{ mol/dm}^3$)

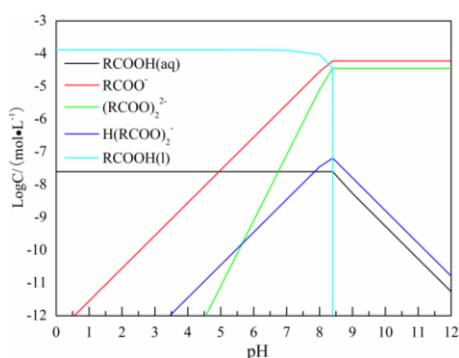


Fig. 9. Species distribution diagrams for oleate ions ($c_{NaOL}=13.16 \times 10^{-5} \text{ mol/dm}^3$)

The “MS+NaOL” addition results in different zeta potential variations in the fluorite and barite flotation systems. The addition of NaOL causes a slight reduction in the zeta potential of the “barite+MS” surface, indicating that NaOL cannot favorably adsorb on the barite surface covered with MS. In the case of fluorite, the decrease for the zeta potential of the “fluorite+MS” surface is noticeable with the addition of NaOL, showing that NaOL can further adsorb on the “fluorite+MS” surface easily. At a pH of 7, the reduction of the “fluorite+MS” surface is 21.2 mV, which is higher than that of the “barite+MS” surface (1.03 mV). This distinction can explain the selective depression for barite with “MS+NaOL” addition (Fig. 4).

To further investigate the behaviors of MS, the addition order of MS and collector in the flotation tests has been changed, and the results are shown in Table 3. It can be noticed that the addition order of MS and NaOL has little effect on the flotation recovery of fluorite. While for barite, the results are quite different, adding sodium oleate first followed by MS can lead to a much higher flotation recovery. The results indicate that MS and NaOL may compete for adsorption on the barite surface. When MS was added first at pH 7, the inhibitor can adsorb on the negative barite surface (Fig. 8(b)), leading to exposing abundant hydroxyl on barite surface and hindering the oleate adsorption. The results also shows that prevent the adsorption of sodium oleate on barite surface is not the only reason for the selective depression of MS.

Table 3. Flotation results of different reagents order tests. (MS: 250 mg/dm³, NaOL: 13.16×10⁻⁵ mol/dm³ at pH 7)

Reagent schedule	Recovery, %
Fluorite + NaOL	92.52
Fluorite + MS + NaOL	88.64
Fluorite + NaOL + MS	89.35
Barite + NaOL	91.16
Barite + MS + NaOL	4.36
Barite + NaOL + MS	52.76

3.5 Contact angle

To further explain the flotation responses of fluorite and barite with MS as a depressant, the wetting behaviors of sodium oleate and MS on the two mineral surfaces were investigated.

The contact angles were measured and the results are presented in Fig. 10. As shown schematically in Fig. 10, the contact angles of fluorite and barite were 43° and 38°, respectively, without flotation reagents. In the presence of 13.16×10⁻⁵ mol/dm³ of sodium oleate, both fluorite and barite showed strong hydrophobic interactions, with the contact angles of the minerals being 106° and 100°, respectively. The results are consistent with references (Gao et al., 2012; Zhang et al., 2015; Kowalczyk and Zawala, 2016; Miller et al., 2016; Kowalczyk et al., 2017). The addition of 250 mg/dm³ of MS resulted in different surface wettability for fluorite and barite. For fluorite, the influence of MS is negligible, as the contact angle decreased from 106° to 102°. The result indicated that MS could slightly reduce the hydrophobicity of fluorite surface. On the other hand, the contact angle of barite decreased from 100° to 57° in the presence of MS, indicating the barite surface hydrophobicity is significantly reduced when MS is added in the flotation system. The contact angle measurement results are consistent with the flotation phenomenon.

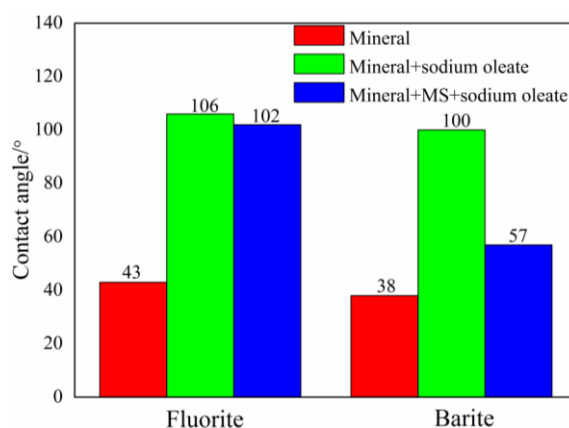


Fig. 10. Contact angle of mineral samples at pH 7

4. Conclusions

The modified starch served as a selective depressant in the separation of fluorite from barite. Flotation tests on a single mineral showed that the modified starch can depress barite selectively. Flotation

results of artificially mixed minerals indicated that the reagent scheme of 250 mg/dm³ of modified starch and 13.16×10⁻⁵ mol/dm³ of sodium oleate at a pH of 7 could obtain selective separation of fluorite from barite. The FTIR spectrum study implied that the modified starch might interact with minerals through forming hydrogen bonds and chemical bonding. Zeta potential analyses revealed that treating the fluorite and barite with modified starch does not preclude sodium oleate from adsorbing onto the fluorite surface, although it prevents sodium oleate from adsorbing on the barite surface. The contact angle measurement results are coherent with the flotation results. Therefore, it can be stated that the modified starch is an appropriate depressant in the selective separation of fluorite from barite using sodium oleate as a collector.

Acknowledgements

The authors would like to acknowledge the financial support by the National Natural Science Foundation of China (51504173) and the Fundamental Research Funds for the Central Universities (WUT: 2016IVA048).

References

- BI K.J., FANG J.J., JIANG T.G., LI G.D., 2015. *Research Status on Flotation Reagents of Barite*. Conservation and Utilization of Mineral Resources, 4, 57- 61.
- CAMBIER P., 1986. *Infrared study of goethites of varying crystallinity and particle size: i. interpretation of oh and lattice vibration frequencies*. Clay Minerals, 21(2), 191-200.
- CHEN T.X., ZHAO Y.L., SONG S.X., 2017. *Electrophoretic mobility study for heterocoagulation of montmorillonite with fluorite in aqueous solutions*. Powder Technology, 309, 61-67.
- GAO Z.Y., BAI D., SUN W., CAO X.F., HU Y.H., 2015 (a). *Selective flotation of scheelite from calcite and fluorite using a collector mixture*. Minerals Engineering, 72, 23-26.
- GAO Z.Y., GAO Y.S., ZHU Y.Y., HU Y.H., SUN W., 2016. *Selective Flotation of Calcite from Fluorite: A Novel Reagent Schedule*. Minerals, 6(4), 114.
- GAO Z.Y., LI C.W., SUN W., HU Y.H., 2017. *Anisotropic surface properties of calcite: A consideration of surface broken bonds*. Colloids and Surfaces A: Physicochemical and Engineering Aspects, 520, 53-61.
- GAO Z.Y., SUN W., HU Y.H., 2014. *Mineral cleavage nature and surface energy: anisotropic surface broken bonds consideration*. Transactions of Nonferrous Metals Society of China, 24(9), 2930-2937.
- GAO Z.Y., SUN W., HU Y.H., 2015 (b). *New insights into the dodecylamine adsorption on scheelite and calcite: an adsorption model*. Minerals Engineering, 79, 54-61.
- GAO Z.Y., SUN W., HU Y.H., LIU X.W., 2012. *Anisotropic surface broken bond properties and wettability of calcite and fluorite crystals*. Transactions of Nonferrous Metals Society of China, 22(5), 1203-1208.
- GOTIĆ M., MUSIĆ S., 2007. *Mössbauer, FT-IR and FE SEM investigation of iron oxides precipitated from FeSO₄ solutions*. Journal of Molecular Structure, 834, 445-453.
- HANNA H.S., 1974. *Adsorption of some starches on spar minerals*. In Recent Advances in Science and Technology of Materials: Springer US, 365- 374.
- HU Y.H., CHI R., XU Z.H., 2003. *Solution Chemistry Study of Salt- type Mineral Flotation Systems: Role of Inorganic Dispersants*. Industrial & Engineering Chemistry Research, 42, 1641-1647.
- KAR B., SAHOO H., RATH S.S., DAS B., 2013. *Investigations on different starches as depressants for iron ore flotation*. Minerals Engineering, 49, 1-6.
- KOMULAINEN S., PURSIAINEN, J., PERÄMÄKI P., LAJUNEN M., 2013. *Complexation of Fe (III) with water-soluble oxidized starch*. Starch-Stärke, 65(3-4), 338-345.
- KOU J., XU S.H., SUN T., SUN C.B., GUO Y., WANG C., 2016. *A study of sodium oleate adsorption on Ca²⁺ activated quartz surface using quartz crystal microbalance with dissipation*. International Journal of Mineral Processing, 154, 24-34.
- KOWALCZUK P.B., AKKAYA C., ERGUN M., JANICKI M.J., SAHBAZ O., DRZYMALA J., 2017. *Water contact angle on corresponding surfaces of freshly fractured fluorite, calcite and mica*. Physicochem. Probl. Miner. Process, 53(1), 192-201.

- KOWALCZUK P.B., ZAWALA J., 2016. *A relationship between time of three-phase contact formation and flotation kinetics of naturally hydrophobic solids*. Colloids and Surfaces A: Physicochemical and Engineering Aspects, 506, 371-377.
- LI H.P., ZHANG S.S., JIANG H., HU Y.H., WANG D.Z., 2010. *Selective depression of diaspore with waxy maize starch*. Minerals Engineering, 23, 1192-1197.
- LI H.P., ZHANG S.S., JIANG H., LI B., 2010. *Effect of modified starches on depression of diaspore*. Transactions of Nonferrous Metals Society of China, 20(8), 1494-1499.
- LU S.S., 2008. *Research on crystal chemistry on flotation of several sulfate minerals*. Northeastern University :Shenyang.
- LU S.S., 2010. *Research on Basic Floatability of Barite and Effect of Fe³⁺ on Which in Sodium Oleate Flotation System*. 8th Annual meeting of China Nonferrous Metals Society, 18-22.
- MILLER J.D., WANG X.M., JIN J.Q., KAUSTUBH SHRIMALI., 2016. *Interfacial water structure and the wetting of mineral surfaces*. International Journal of Mineral Processing, 156, 62-68.
- NUNES A., PERES A., DE ARAUJO A., GEORGE EDUARDO SALES VALADAO., 2011. *Electrokinetic properties of wavellite and its floatability with cationic and anionic collectors*. Journal of Colloid and Interface Science, 361(2), 632- 638.
- RAO K., CASES J., DE DONATO P., K.S.E. FORSSBERG., 1991. *Mechanism of Oleate Interaction on Salt- Type Minerals*. Journal of Colloid and Interface Science, 145(2), 314- 329.
- REN Z.J., YU F.T., GAO H.M., CHEN Z.J., PENG Y.J., LIU L.Y., 2017. *Selective Separation of Fluorite, Barite and Calcite with Valonea Extract and Sodium Fluosilicate as Depressants*. Minerals, 7(2), 24.
- UCAR A., ÖZDAG H., 2013. *Mechanism of collector adsorption in fluorite flotation*. Mineral Processing and Extractive Metallurgy Review, 100-105.
- WANG G.J., 2013. *Research on mechanism and application of several kinds of modified starch as hematite inhibitor*. Central South University: Changsha.
- WANG J.J., GAO Z.Y., GAO Y.S., HU Y.H., SUN W., 2016. *Flotation separation of scheelite from calcite using mixed cationic/anionic collectors*. Minerals Engineering, 98, 261-263.
- WEN L., 1989. *Mineral Infrared Spectroscopy*. Chongqing: Chongqing University Press.
- XIA L.Y., ZHONG H., LIU G.Y., WANG S., 2009. *Utilization of soluble starch as a depressant for the reverse flotation of diaspore from kaolinite*. Minerals Engineering, 22, 560-565.
- XU L.H., DONG F.Q., WU H.Q., WANG Z., XIAO J.H., 2013. *A Study on Spodumene Flotation Mechanism by Sodium Oleate*. Acta Mineralogica Sinica, 33(2), 181.
- XU L.H., HU Y.H., WU H.Q., TIAN J., LIU J., GAO Z.Y., WANG L., 2016. *Surface crystal chemistry of spodumene with different size fractions and implications for flotation*. Separation and Purification Technology, 169, 33-42.
- YU F.T., 2015. *Study on Flotation Behavior of Fluorite, Barite and Calcite in Wuling Mountainous Area*. Wuhan University of Technology: Wuhan.
- YU X.Y., ZENG A., WANG H.L., WANG Q.Q., WEI X.A., 2016. *Preparation method of flotation depressant and its application*. C.N. Patent 201610045869. 7.
- ZHANG B., LI J., ZHANG X.F., CAO Z., WANG J.L., HAN H., 2016. *Activation and mechanism of Cu²⁺ and Fe³⁺ in flotation system of fluorite ore*. Chinese Journal of Rare Metals, 40(9), 963- 968.
- ZHANG X., WANG X.M., JAN D. MILLER., 2015. *Wetting of selected fluorite surfaces by water*. Surface Innovations, 3(1), 39-48.